Table III. Selected Bond Distances and Angles for $[PPN]_2[Os_3Ni_4C(CO)_{15}]$

	Bond Distances (Å)		
Os1–C	2.09 (2)	Ni2–C	1.97 (2)
Os2–C	2.08 (2)	Ni3–C	1.94 (2)
Os3···C	2.76 (2)	Ni4–C	1.94 (2)
Ni1–C	1.95 (2)		
Ni1–Ni2	2.392 (3)	Ni2–Ni3	2.542 (4)
Ni1–Ni4	2.560 (4)	Ni3–Ni4	2.382 (3)
Os1–Os2	2.888 (1)	Os2–Ni1	2.733 (3)
Os1–Os3	2.804 (1)	Os2–Ni4	2.695 (3)
Os1–Ni2	2.715 (3)	Os3–Ni3	2.760 (3)
Os1–Ni3	2.688 (3)	Os3–Ni4	2.757 (3)
Os2–Os3	2.809 (2)		
	Bond Angles (deg)		
Os2–Os1–Os3	59.12 (4)	Os2–Ni1–Ni2	95.1 (1)
Os2–Os1–Ni2	84.97 (6)	Os2–Ni1–Ni4	61.10 (8)
Os2–Os1–Ni3	84.51 (6)	Ni2–Ni1–Ni4	90.3 (1)
Os3–Os1–Ni2	108.32 (7)	Os1–Ni2–Ni1	95.4 (1)
Os3–Os1–Ni3	60.28 (6)	Os1–Ni2–Ni3	61.39 (8)
Ni2–Os1–Ni3	56.12 (8)	Ni1–Ni2–Ni3	89.5 (1)
Os1–Os2–Os3	58.95 (4)	Os1–Ni3–Os3	61.96 (6)
Os1–Os2–Ni1	84.56 (6)	Os1–Ni3–Ni2	62.49 (9)
Os1–Os2–Ni4	84.69 (6)	Os1–Ni3–Ni4	95.7 (1)
Os3–Os2–Ni1	107.85 (7)	Os3–Ni3–Ni4	64.37 (9)
Os3–Os2–Ni4	60.08 (6)	Ni2–Ni3–Ni4	90.9 (1)
Ni1–Os2–Ni4	56.27 (8)	Os2–Ni4–Os3	62.02 (6)
Os1–Os3–Os2	61.93 (4)	Os2–Ni4–Ni1	62.63 (9)
Os1–Os3–Ni3	57.77 (6)	Os2–Ni4–Ni3	95.1 (1)
Os1–Os3–Ni4	85.16 (6)	Os3–Ni4–Ni1	114.8 (1)
Os2–Os3–Ni3	84.72 (7)	Os3–Ni4–Ni3	64.47 (9)
Os2–Os3–Ni4	57.89 (6)	Ni1–Ni4–Ni3	89.3 (1)
Ni3–Os3–Ni4	51.15 (7)		

(1) Å),[16] respectively. Ni–C distances are comparable to those found in $[PPN]_2[Ru_3Ni_3C(CO)_{13}]$ (1.85 (1)–1.96 (1) Å)[8] and $[Ni_7C(CO)_{12}]^{2-}$, although in $[Ni_7C(CO)_{12}]^{2-}$ the carbide appears to be bonded to all seven nickel atoms (Ni_{cap}–C = 1.95 Å, Ni–Ni 1.94–2.09 Å).[14] Os–C distances are similar to those in $[Os_{10}C(CO)_{24}]^{2-}$ (mean 2.04 (3) Å)[15] and $[Os_6C(CO)_{16}(MeCCMe)]$ (mean 2.04 (2) Å).[17]

The solution ^{13}C NMR spectra of II are consistent with its solid-state structure. The carbide resonance occurs at 333.5 ppm. Peaks at 256.3 and 210.4 ppm may be assigned to the bridging carbonyls on the Ni atoms. Resonances at 209.2 and 209.1 ppm are assigned to the terminal carbonyls on the Ni atoms, and those at 194.4 and 184.3 ppm belong to terminal carbonyls on the Os atoms. A plane of symmetry runs through the capping Os perpendicular to the square faces of the trigonal prism for the static molecule. Broadening of the carbonyl resonances at 20 °C indicates that exchange of all carbonyls occurs at elevated temperatures. At −90 °C, broadening of resonances at 194.4 and 184.3 ppm indicates slowing of intrametal CO exchange.

The geometry of II may be viewed as a condensation of a trigonal prism (90 e) and a square pyramid (74 e) sharing a square face (64 e).[18] Thus, II is expected by PSEPT to have 100 electrons, 90 + 74 − 64, and is electron precise. Although other geometries are more common, four other clusters are known to adopt this same metal configuration.[14,18]

Factors determining the geometry of a cluster include its electron count[1,4] and the site preferences of interstitial atoms.[19] Other observed geometries for seven-metal clusters include a trigonal prism capped on a triangular face (102 e), a capped octahedron (98 e), an edge-bridged capped square pyramid (100 e), an edge-bridged octahedron (100 e), and a tricapped tetrahedron (96 e).[1] Unlike many mixed-metal clusters containing Pt metals, II adopts a geometry expected for its electron count. Clusters with Ni are more often electron precise than those with Pd or Pt, however.[1] In compound II, the Os atom prefers the capping site of the cluster, although it might be expected that, in the formation of a heptametallic cluster, nickel might cap one face, leaving all three Os–carbide bonds intact. Apparently, under the synthetic conditions, site preferences of the metal atoms, rather than kinetic factors, determine the final metal arrangement.

It has been suggested that in heterometallic clusters M–L and M–M bond strengths determine thermodynamic metal site preferences.[19] When M–L bonding does not vary between the alternative metal arrangements, the structure which maximizes the total M–M bond strength is favored. Heats of vaporization indicate that the average M–M bond strength in the metal, $\bar{M}$, is greater for osmium than for nickel (Ni, $\bar{M}$ = 71 kJ/mol; Os, $\bar{M}$ = 132 kJ/mol).[20,21] The configuration of metals found in II maximizes Os–Os and Os–Ni bonding, at the expense of weaker Ni–Ni bonding.

Acknowledgment. This research was supported by the U.S. Department of Energy, Organometallic and Surface Chemistry Program (Grant DE-FG02-86ER13640).

Supplementary Material Available: Full lists of positional parameters and bond distances and angles (13 pages); a structure factor table (69 pages). Ordering information is given on any current masthead page.

---

(16) Farrugia, L. J.; Howard, J. A. K.; Mitrprachachon, P.; Stone, F. G. A.; Woodward, P. *J. Chem. Soc., Dalton Trans.* **1981**, 171.

(17) Eady, C. R.; Fernandez, J. M.; Johnson, B. F. G.; Lewis, J.; Raithby, P. R.; Sheldrick, G. M. *J. Chem. Soc., Chem. Commun.* **1978**, 421.

(18) Martinengo, S.; Ciani, G.; Sironi, A. *J. Chem. Soc., Chem. Commun.* **1984**, 1577.

(19) Mingos, D. M. P.; Zhenyeng, L. *Comments Inorg. Chem.* **1989**, *9*, 95.

(20) Connor, J. A. In *Transition Metal Clusters*; Johnson, B. F. G., Ed.; Wiley: New York, 1980; p 345.

(21) Mingos, D. M. P.; Wales, D. J. *Introduction to Cluster Chemistry*; Wiley: New York, 1990; p 8.

Contribution from the Department of Chemistry
and Biochemistry, University of Notre Dame,
Notre Dame, Indiana 46556,
and Laboratoire de Chimie de Coordination,
Unité de Recherche Associée au CNRS No. 1194,
Département de Recherche Fondamentale, Centre d'Études
Nucléaires de Grenoble, 38041 Grenoble Cedex, France

Two Salts of Bis(ethanol)(*meso*-tetraphenylporphinato)iron(III). Molecular Structures and Magnetic Susceptibilities

W. Robert Scheidt,*[1a] David K. Geiger,[1a,b] Young Ja Lee,[1a] Pierre Gans,[1c] and Jean-Claude Marchon*[1c]

Received September 9, 1991

Six-coordinate iron(III) porphyrinates with neutral, weak-field, oxygen donor axial ligands have been generally found to have an $S = {}^5/_2$ (high-spin) ground state.[2,3] Interestingly, Gans et al. have synthesized and characterized a bis(ethanol) complex of $Fe^{III}TPP$ that *almost* fits this pattern.[4] This species, $[Fe(TPP)(EtOH)_2]BF_4$,[5] has been described by a quantum mechanical admixture of spin quartet ($S = {}^3/_2$) and spin sextet ($S = {}^5/_2$) states, with the sextet lying about 200 cm^{-1} lower.[6] This

---

(1) (a) University of Notre Dame. (b) Present address: Department of Chemistry, SUNY-Geneseo, Geneseo, NY 14454. (c) Centre d'Études Nucléaires de Grenoble.

(2) Scheidt, W. R.; Reed, C. A. *Chem. Rev.* **1981**, *81*, 543.

(3) (a) Mashiko, T.; Kastner, M. E.; Spartalian, K.; Scheidt, W. R.; Reed, C. A. *J. Am. Chem. Soc.* **1978**, *100*, 6354. (b) Scheidt, W. R.; Cohen, I. A.; Kastner, M. E. *Biochemistry* **1979**, *18*, 3546.

(4) Gans, P.; Buisson, G.; Duée, E.; Regnard, J.-R.; Marchon, J.-C. *J. Chem. Soc., Chem. Commun.* **1979**, 393.

(5) Abbreviations used: TPP and OEP, dianions of *meso*-tetraphenylporphyrin and octaethylporphyrin; EtOH, ethanol; THF, tetrahydrofuran; TMSO, tetramethylene sulfoxide.

0020-1669/92/1331-2660$03.00/0 © 1992 American Chemical Society

Table I. Summary of Crystal Data and Intensity Collection Parameters

	$[Fe(TPP)(EtOH)_2]ClO_4$	$[Fe(TPP)(EtOH)_2]BF_4$
formula	$FeClO_6N_4C_{48}H_{40}$	$FeF_4O_2N_4C_{48}BH_{40}$
fw, amu	860.17	847.52
temp, K	292	99
a, Å	10.600 (5)	10.447 (4)
b, Å	16.792 (4)	16.612 (6)
c, Å	11.963 (2)	11.798 (5)
β, deg	108.79 (1)	108.65 (3)
V, Å^3	2015.9	1939.9
Z	2	2
space group	$P2_1/n$	$P2_1/n$
d_{calcd}, g/cm^3	1.42	1.45
d_{meas}, g/cm^3	1.41	1.39[a]
radiation	graphite-monochromated Mo Kα (λ = 0.71073 Å)	
μ, mm^{-1}	0.49	0.45
R_1	0.055	0.057
R_2	0.071	0.061
goodness of fit	2.03	1.64

[a] Measured at 292 K.

unusual magnetic behavior has led us to further investigate the bis(ethanol)-ligated iron(III) system. We have characterized a species that differs "only" by a change of the counteranion to perchlorate; this species shows simple high-spin magnetic behavior over the entire temperature range 4.5–300 K. We have also investigated the structure of the first (BF_4^-) salt at lower (99 K) temperature and reinvestigated its magnetic properties with a SQUID susceptometer over the temperature range 2–300 K. We report herein the results of these studies and our interpretation of the differing physical properties of the two salts.

Experimental Section

Syntheses. The $[Fe(TPP)]_2O$ starting material was twice chromatographed on basic alumina (Woelm, Akt. 1) with CH_2Cl_2 as eluent.

$[Fe(TPP)(EtOH)_2]BF_4$. A 1-g sample of $[Fe(TPP)]_2O$ was dissolved in 250 mL of a chloroform–ethanol (40:1) mixture. To the greenish-brown solution was added 1 mL of a 33% aqueous HBF_4 solution, whereupon the color turned red. After being stirred for 30 min, the mixture was evaporated to dryness; the solid residue was taken up in 20 mL of CH_2Cl_2, and 50 mL of cyclohexane was added. A 831-mg (66%) yield of blue crystals were obtained by filtration after 5 days. Mass spectrum, m/e (ion): 46 ($C_2H_5OH^+$), 79 ($BF_2OCH_2^+$), 93 ($BFOC_2H_4^+$), 105 ($BFOCH_2OEt^+$), 120 ($BFO_2Et_2^+$), 668 ($FeTPP^+$). IR, KBr pellet: 1035, 1085, 1125 cm^{-1} (ν_{B-F}).[7] UV–vis, ethanol solution λ_{max} nm (ϵ, 10^3 L·mol^{-1}·cm^{-1}): 395 (120), 500 (10), 531 (12.6), 655 (2.4), 690 (2.5); Anal. Calcd for $FeF_4O_2N_4C_{48}H_{40}$: C, 68.03; H, 4.76; N, 6.61; Fe, 6.59; F, 8.97; B, 1.28. Found: C, 67.71; H, 4.76; N, 6.55; Fe, 6.64; F, 9.12; B, 1.14.

$[Fe(TPP)(EtOH)_2]ClO_4$. A 950-mg sample of $[Fe(TPP)]_2O$ was dissolved in 200 mL of a dichloromethane–ethanol (1:1) mixture, and 1 mL of a 70% aqueous $HClO_4$ solution was added dropwise. After the red solution was stirred for 30 min, the solvent mixture was slowly evaporated under reduced pressure until crystallization started. The solution was left still for 1 week, and the resulting blue crystals (860 mg, 71%) were collected by filtration. Anal. Calcd for $FeClO_6N_4C_{48}H_{40}$: C, 67.03; H, 4.69; N, 6.51; Fe, 6.49; Cl, 4.12. Found: C, 64.00; H, 4.55; N, 6.22; Fe, 6.20; Cl, 5.33. The presence of ethanol was confirmed by the appearance of a peak at m/e 46 in the mass spectrum.

Magnetic Measurements. Variable-temperature magnetic susceptibility data for the tetrafluoroborate salt were obtained between 2 and 300 K by using a SQUID susceptometer (Quantum Design, MPMS) operating at 5 kG, whereas data on the perchlorate salt were obtained between 4.5 and 300 K on a SQUID susceptometer (SHE Corp, VTS 905) operating at 5 kG. The crystalline sample of the tetrafluoroborate salt was finely ground, and the magnetic susceptibility measurements were started at 2 K to avoid possible orientation effects. All data were corrected for diamagnetism and are reported as effective magnetic moments.

Structural Characterization. Both crystalline species were examined on a Nicolet P$\bar{1}$ diffractometer. Least-squares refinement of the setting angles of 60 reflections, collected at $\pm 2\theta$, gave the cell constants reported in Table I. Complete details of the intensity data collection parameters and refinement are given in Table I. Low-temperature measurements for $[Fe(TPP)(EtOH)_2]BF_4$ were made using a locally modified LT-1 low-temperature attachment for the diffractometer. Data were reduced as previously described.[8] Most atomic positions for $[Fe(TPP)(EtOH)_2]ClO_4$ were obtained from the direct methods program MULTAN.[9] Subsequent difference Fourier syntheses gave positions for the perchlorate anion, missing phenyl carbon atoms, and the disordered carbon atoms of the ethanol ligand. Trial coordinates for $[Fe(TPP)(EtOH)_2]BF_4$ were taken from final coordinates of $[Fe(TPP)(EtOH)_2]ClO_4$.

Table II. Fractional Coordinates for $[Fe(TPP)(EtOH)_2]ClO_4$[a]

atom	x	y	z
Fe	0.0	0.0	0.0
Cl	0.5000	0.0	0.0
O(1)	−0.16634 (17)	0.06882 (11)	0.00738 (17)
N(1)	−0.01537 (18)	0.04962 (11)	−0.16020 (16)
N(2)	0.12492 (18)	0.08822 (11)	0.08221 (16)
C(a1)	−0.09731 (22)	0.02399 (14)	−0.26915 (19)
C(a2)	0.04266 (21)	0.11950 (13)	−0.17958 (20)
C(a3)	0.16179 (22)	0.15331 (14)	0.02936 (21)
C(a4)	0.17764 (22)	0.10018 (14)	0.20292 (20)
C(b1)	−0.09120 (24)	0.08094 (15)	−0.35752 (20)
C(b2)	−0.00403 (23)	0.13827 (14)	−0.30284 (21)
C(b3)	0.23431 (26)	0.20842 (15)	0.11942 (23)
C(b4)	0.24351 (26)	0.17636 (15)	0.22460 (22)
C(m1)	−0.17137 (21)	−0.04636 (13)	−0.29104 (19)
C(m2)	0.12937 (21)	0.16694 (13)	−0.09205 (20)
C(1)	−0.25396 (24)	−0.06630 (14)	−0.41506 (20)
C(2)	−0.39038 (25)	−0.07940 (16)	−0.44151 (22)
C(3)	−0.46830 (28)	−0.09878 (19)	−0.55493 (27)
C(4)	−0.4137 (3)	−0.10543 (20)	−0.64338 (26)
C(5)	−0.2802 (3)	−0.09198 (19)	−0.61962 (24)
C(6)	−0.19955 (26)	−0.07299 (16)	−0.50627 (22)
C(7)	0.19302 (22)	0.23805 (13)	−0.12797 (19)
C(8)	0.12062 (27)	0.30630 (16)	−0.17172 (25)
C(9)	0.1814 (3)	0.37325 (16)	−0.19915 (28)
C(10)	0.3159 (3)	0.37159 (18)	−0.18443 (26)
C(11)	0.38854 (29)	0.30398 (19)	−0.14326 (28)
C(12)	0.32773 (25)	0.23736 (16)	−0.11448 (24)
C(13a)	−0.2123 (8)	0.1438 (5)	−0.0557 (7)
C(13b)	−0.1695 (10)	0.1564 (5)	0.0135 (11)
C(14a)	−0.1965 (23)	0.2038 (12)	0.0337 (14)
C(14b)	−0.2833 (10)	0.1973 (7)	−0.0037 (11)
O(2)	0.3618 (5)	0.0068 (3)	−0.0809 (5)
O(3)	0.5213 (9)	0.0893 (4)	0.0358 (9)
O(4)	0.5692 (9)	−0.0171 (10)	−0.0792 (12)
O(5)	0.5041 (15)	−0.0386 (7)	0.0891 (10)

[a] The estimated standard deviations of the least significant digits are given in parentheses.

The two-molecule unit cells and the uniquely defined space group requires that the $[Fe(TPP)(EtOH)_2]^+$ ions and the perchlorate or tetrafluoroborate anions possess inversion symmetry. Thus, the anions must be disordered around an inversion center (at $^1/_2$, 0, 0). Close examination of difference Fourier maps led to placing the boron atom at 0.5155, −0.0122, 0.0060, while the chlorine atom was placed at $^1/_2$, 0, 0. Each central atom was held at a fixed position and given an occupancy factor of 0.5. The coordinates of the four attached atoms (F or O) were allowed to vary; the occupancies were fixed at 0.5. There are thus two orientations of each anion; the total retains the required inversion symmetry. The model used for the disordered ethanol ligands allowed two positions for each of the carbon atoms with the occupancy factor sum of each type constrained to unity. Full-matrix least-squares refinement, followed by a difference Fourier synthesis, led to location of all hydrogen atoms. These hydrogen atom positions were idealized (C–H = 0.95 Å, B(H) = B(C) + 1.0 Å^2) and included as fixed contributors in all subsequent refinement cycles. Refinement was then carried to convergence to yield

---

(6) Regnard, J. R.; Gans, P. *Hyperfine Interact.* **1986**, *29*, 1435.

(7) Gaughan, A. P., Jr.; Dori, Z.; Ibers, J. A. *Inorg. Chem.* **1974**, *13*, 1657.

(8) Scheidt, W. R. *J. Am. Chem. Soc.* **1974**, *96*, 84.

(9) Programs used in this study included local modifications of Main, Hull, Lessinger, Germain, Declerq, and Woolfson's MULTAN, Jacobson's ALLS, Zalkin's FORDAP, Busing and Levy's ORFFE and ORFLS, and Johnson's ORTEP2. Atomic form factors were from: Cromer, D. T.; Mann, J. B. *Acta Crystallogr., Sect. A* **1968**, *A24*, 321. Real and imaginary corrections for anomalous dispersion in the form factor of the iron and chlorine atoms were from: Cromer, D. T.; Liberman, D. J. *J. Chem. Phys.* **1970**, *53*, 1891. Scattering factors for hydrogen were from: Stewart, R. F.; Davidson, E. R.; Simpson, W. T. *J. Chem. Phys.* **1965**, *42*, 3175. All calculations were performed on VAX 11/730 or 3200 computers.

Table III. Fractional Coordinates for $[Fe(TPP)(EtOH)_2]BF_4$ at 99 K[a]

atom	*x*	*y*	*z*
Fe	0.0	0.0	0.0
O	−0.16676 (18)	0.07032 (11)	0.00561 (18)
N(1)	−0.01483 (20)	0.04999 (12)	−0.16258 (19)
N(2)	0.12832 (21)	0.08907 (12)	0.08386 (19)
C(a1)	−0.09775 (25)	0.02453 (15)	−0.27322 (23)
C(a2)	0.04535 (24)	0.12048 (15)	−0.18207 (22)
C(a3)	0.16454 (25)	0.15553 (15)	0.03026 (24)
C(a4)	0.17987 (25)	0.10130 (15)	0.20543 (23)
C(b1)	−0.09186 (25)	0.08167 (15)	−0.36280 (23)
C(b2)	−0.00199 (25)	0.13918 (15)	−0.30689 (24)
C(b3)	0.23574 (26)	0.21135 (16)	0.12078 (25)
C(b4)	0.24365 (27)	0.17904 (16)	0.22739 (24)
C(m1)	−0.17384 (25)	−0.04698 (15)	−0.29484 (22)
C(m2)	0.13292 (24)	0.16850 (15)	−0.09305 (23)
C(1)	−0.25789 (25)	−0.06644 (15)	−0.42062 (23)
C(2)	−0.39612 (27)	−0.08131 (16)	−0.44505 (25)
C(3)	−0.47733 (28)	−0.10134 (19)	−0.56005 (27)
C(4)	−0.4230 (3)	−0.10489 (18)	−0.65198 (26)
C(5)	−0.28647 (29)	−0.08915 (17)	−0.62950 (25)
C(6)	−0.20435 (26)	−0.07095 (15)	−0.51429 (24)
C(7)	0.19666 (26)	0.24028 (15)	−0.12954 (23)
C(8)	0.12151 (27)	0.30845 (16)	−0.17752 (25)
C(9)	0.1826 (3)	0.37633 (17)	−0.20552 (26)
C(10)	0.3199 (3)	0.37621 (17)	−0.18773 (26)
C(11)	0.39501 (28)	0.30848 (18)	−0.14222 (26)
C(12)	0.33573 (26)	0.24084 (16)	−0.11183 (25)
C(13a)	−0.2131 (6)	0.1447 (4)	−0.0544 (6)
C(13b)	−0.1571 (6)	0.1602 (4)	0.0177 (6)
C(14a)	−0.2923 (5)	0.1965 (4)	−0.0036 (7)
C(14b)	−0.2162 (20)	0.2059 (8)	0.0290 (11)
B	0.5155	−0.0112	0.0060
F(1)	0.6451 (3)	−0.00030 (22)	0.08168 (29)
F(2)	0.5043 (6)	−0.08514 (27)	−0.0449 (5)
F(3)	0.4269 (4)	−0.0057 (5)	0.0709 (4)
F(4)	0.4823 (5)	0.04516 (28)	−0.0824 (4)

[a] The estimated standard deviations of the least significant digits are given in parentheses.

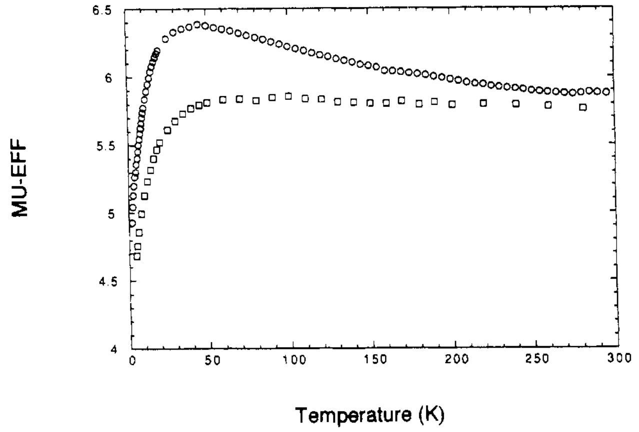

Figure 1. Temperature dependence of the effective magnetic moments of $[Fe(TPP)(EtOH)_2]BF_4$ (○) and $[Fe(TPP)(EtOH)_2]ClO_4$ (□).

the *R* values recorded in Table I. Final atomic coordinates are listed in Tables II and III. Anisotropic thermal parameters and fixed hydrogen atom coordinates are available as supplementary material.

Results

Magnetic Properties. $[Fe(TPP)(EtOH)_2]ClO_4$ shows simple high-spin behavior in the temperature range 4.5 to 300 K. Linear regression of a plot of $1/\chi_M$ vs T gave a magnetic moment of 5.8 μ_B and a Weiss temperature of −1 K. $[Fe(TPP)(EtOH)_2]BF_4$ shows similar behavior at room temperature (magnetic moment 5.8 μ_B) but then shows a slowly increasing magnetic moment (up to 6.3 μ_B) as the temperature is decreased down to 45 K. This suggests some ferromagnetic ordering of the iron(III) spins along the hydrogen-bonded chains (see below). Plots of the temperature-dependent effective magnetic moments for the two salts of $[Fe(TPP)(EtOH)_2]^+$ are shown in Figure 1. The similarity of behavior at room temperature and the differences at lower temperatures are apparent.

Table IV. Comparison of Selected Bond Distances in $[Fe(TPP)(EtOH)_2]^+$ Derivatives[a]

	$[Fe(TPP)(EtOH)_2]ClO_4$	$[Fe(TPP)(EtOH)_2]BF_4$	$[Fe(TPP)(EtOH)_2]BF_4$
temp	room temp	room temp	99 K
$Fe-N_1$	2.048 (2)	2.035 (6)	2.050 (2)
$Fe-N_2$	2.019 (2)	2.019 (5)	2.029 (2)
Fe–O	2.134 (2)	2.142 (9)	2.116 (2)
ref	this work	4	this work

[a] Numbers in parentheses are estimated standard deviations for individual values.

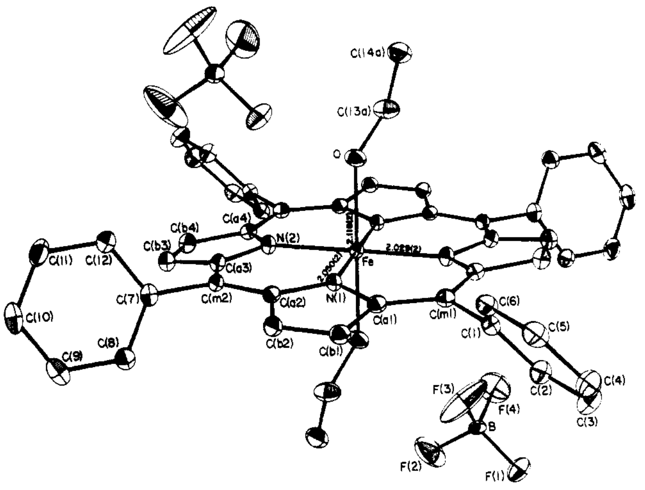

Figure 2. ORTEP drawing of the structure of the $[Fe(TPP)(EtOH)_2]BF_4$ derivative at 99 K. Ellipsoid surfaces are contoured at the 50% probability level. Atom labels are given for the crystallographically unique atoms of the ion.

X-ray Structures. The perchlorate and tetrafluoroborate salts of the $[Fe(TPP)(EtOH)_2]^+$ cation crystallize in the same monoclinic space group. The cation and anion each have crystallographically required inversion symmetry. $[Fe(TPP)(EtOH)_2]ClO_4$ is found to have two nonequivalent $Fe-N_p$ bonds, with distances of 2.048 (2) and 2.019 (2) Å. These values are similar to those seen in the room-temperature structure of $[Fe(TPP)(EtOH)_2]BF_4$,[4] i.e., both in magnitude and in orientation with respect to the unit cell vectors. The structure of the BF_4^- salt, determined at 99 K, was also found to retain this rhombicity in the equatorial $Fe-N_p$ bonds although the bonds appear to have increased in length. A comparison of selected bond distances and angles for these two new structure determinations with those of the room-temperature form of the BF_4^- salt is given in Table IV. Figure 2 displays the structure of $[Fe(TPP)(EtOH)_2]BF_4$ at 90 K and shows the common labeling scheme used in all structures. Figure S1 displays the molecular structure of $[Fe(TPP)(EtOH)_2]ClO_4$ and shows the nature of the disorder found for the carbon atoms of the axial ligand. This disorder is also seen and resolved in the 99 K structure of $[Fe(TPP)(EtOH)_2]BF_4$. The average $Fe-N_p$ bond distances are slightly shorter than those of known high-spin derivatives: 2.045 Å in both $[Fe(TPP)(TMSO)_2]^+$ and $[Fe(TPP)(H_2O)_2]^{+3}$ but significantly longer than that found (1.978 Å)[10] in the admixed intermediate-spin derivative $[Fe(OEP)(THF)_2]^+$. They are similar to that (2.034 Å) seen[11] in the derivative $[Fe(OEP)(EtOH)_2]^+$; unfortunately, there are no magnetic data available for this particular solvate of the complex and the spin state is unknown.

---

(10) Masuda, H.; Taga, T.; Osaki, K.; Sugimoto, H.; Yoshida, Z.-I.; Ogoshi, H. *Bull. Chem. Soc. Jpn.* **1982**, *55*, 3891.

(11) Einstein, F. W. B.; Willis, A. C. *Inorg. Chem.* **1978**, *17*, 3040.

The unique bond length to the axial ligand (Table IV) is significantly longer than the 2.087 (3) Å found[3a] for $[\mathrm{Fe(TPP)(TMSO)_2}]^+$ or the 2.095 (2) Å value found[3b] for $[\mathrm{Fe(TPP)(H_2O)_2}]^+$, both of which are high-spin species, but shorter than the 2.187 (11) Å value found[10] for the admixed intermediate-spin complex $[\mathrm{Fe(OEP)(THF)_2}]^+$.

Averaged values of bond distances and angles in the porphinato core are given in Table IV; no unusual values are noted. Individual values of distances and angles are available as supplementary material. The hydroxylic hydrogen atom of the axial ethanol ligands are hydrogen bonded to the anion in both complexes. In $[\mathrm{Fe(TPP)(EtOH)_2}]\mathrm{BF_4}$, the oxygen to fluoride distance is either 2.68 or 2.79 Å at 99 K. These values are in good agreement with the O···F of 2.702 and 2.753 Å found in the structure of $[(\mathrm{CH_3OH})_2\mathrm{H}]\mathrm{BF_4}$ at −50 °C.[12] The corresponding O···O distances in $[\mathrm{Fe(TPP)(EtOH)_2}]\mathrm{ClO_4}$ are significantly longer at either 2.80 or 3.02 Å at 292 K. In both salts, the hydrogen bond distance depends on which anion orientation is closest to the ethanol oxygen atom, but all ethanol ligands are hydrogen bonded to an anion. This hydrogen bond network leads to a linear chain of alternating cations and anions in the crystal lattice.

Discussion

Crystalline $[\mathrm{Fe(TPP)(EtOH)_2}]\mathrm{ClO_4}$ is found not only to be isomorphous with $[\mathrm{Fe(TPP)(EtOH)_2}]\mathrm{BF_4}$ but also to show very similar structural features. A particularly interesting and unexpected feature is the rhombicity in the Fe–$\mathrm{N_p}$ bond lengths. This rhombicity is seen in both the room- and low-temperature crystal structures of $[\mathrm{Fe(TPP)(EtOH)_2}]\mathrm{BF_4}$ and in the room-temperature crystal structure of $[\mathrm{Fe(TPP)(EtOH)_2}]\mathrm{ClO_4}$. The axial Fe–O bond lengths in the two complexes are also similar. These observations do not allow for an explanation of the differing temperature-dependent effective magnetic moments of $[\mathrm{Fe(TPP)(EtOH)_2}]\mathrm{ClO_4}$ and $[\mathrm{Fe(TPP)(EtOH)_2}]\mathrm{BF_4}$ on an obvious structural basis at the coordination group level.

We believe that the presence or absence of ferromagnetic ordering in the two salts arise from subtle differences in the hydrogen bonding between the ethanol ligands and the anion. With identical O–H donors and quite similar O and F acceptors, the lengths of the O–H–O and O–H–F hydrogen bonds are expected to be the same.[13] However, as noted in the Results, the O–H–O hydrogen bond lengths in the perchlorate salt are significantly longer than the O–H–F lengths in the tetrafluoroborate salt, and hence hydrogen bonding is slightly stronger in the latter. Previous evidence for the ready change of magnetic properties of the bis(aquo)iron(III) or the bis(ethanol)iron(III) system may be found from the reports of Scheidt and Reed,[2,14] Mitra et al.,[15] and Dolphin et al.[16] Mitra et al. report a $[\mathrm{Fe(TPP)(EtOH)_2}]^+$ complex with a magnetic moment substantially reduced from that expected for a high-spin complex, while Dolphin reports a $[\mathrm{Fe(OEP)(EtOH)_2}]^+$ complex with a very large Mössbauer quadrupole doublet. Unfortunately, neither bis(ethanol)iron(III) system has been characterized sufficiently to allow us to comment on any structural basis for their apparent differing magnetic properties. In the present case, however, it appears that the two salts have similar spin ground states but that they differ in their bulk magnetic properties because of small differences in the hydrogen bonding between ligand and anion.

Acknowledgment. We thank the National Institutes of Health (Grant GM-38401 to W.R.S.) and the Centre National de la Recherche Scientifique (URA 1194) for support of this research. We thank Jean-François Jacquot for his help with the SQUID measurements.

Supplementary Material Available: Figure S1, an ORTEP plot illustrating the disorder in the carbon positions of the axial ethanol ligands in $[\mathrm{Fe(TPP)(EtOH)_2}]\mathrm{ClO_4}$, Tables SI, SII, SV, and SVI, giving anisotropic thermal parameters, fixed hydrogen atom positions, bond distances, and angles for $[\mathrm{Fe(TPP)(EtOH)_2}]\mathrm{ClO_4}$, Tables SIII, SIV, SVII, and SVIII, giving anisotropic thermal parameters, fixed hydrogen atom positions, bond distances, and bond angles for $[\mathrm{Fe(TPP)(EtOH)_2}]\mathrm{BF_4}$, and Table SIX, giving complete crystallographic details (10 pages); listings of observed and calculated structure amplitudes (×10) (28 pages). Ordering information is given on any current masthead page.

---

(12) Mootz, D.; Steffen, M. *Angew. Chem., Int. Ed. Engl.* **1981**, *20*, 196.

(13) Ibers, J. A.; Hamilton, W. C. *Hydrogen Bonding in Solids*; W. A. Benjamin; New York, NY, 1968; Table 1-1.

(14) Reed, C. A.; Mashiko, T.; Bentley, S. P.; Kastner, M. E.; Scheidt, W. R.; Spartalian, K.; Lang, G. *J. Am. Chem. Soc.* **1979**, *101*, 2948.

(15) Mitra, S.; Date, S. K.; Nipankar, S. V.; Birdy, R.; Girerd, J.-J. *Proc.—Indian Acad. Sci.* **1980**, *89*, 511.

(16) Dolphin, D. H.; Sams, J. R.; Tsin, T. B. *Inorg. Chem.* **1978**, *17*, 711.

Contribution from the Department of Chemistry,
P.O. Box 3055, University of Victoria,
Victoria, BC, Canada V8W 3P6

Evidence for Ligand Isomerism in the Palladium(II) Complex of 1,4,7-Trithiacyclodecane

S. Chandrasekhar and A. McAuley*

Received July 13, 1991

Interest in homoleptic transition-metal complexes containing crown thioether ligands has seen significant increase only in the past five years.[1-15] Like the triaza macrocyclic analogues, trithia systems such as [9]-ane$\mathrm{S_3}$ (**1**) provide examples of complexes where less common higher and lower oxidation states have been identified. Particular attention has been paid to weak interactions in axial sites of $\mathrm{d^8}$ ions.[16] In the case of palladium(II), comment has been made[6,7,17] on the $[\mathrm{S_4} + \mathrm{S_2}]$ configuration where four

---

(1) Setzer, W. N.; Ogle, C. A.; Wilson, G. S.; Glass, R. S. *Inorg. Chem.* **1983**, *22*, 266.

(2) Wieghardt, K.; Küppers, H. J.; Weiss, H. Z. *Inorg. Chem.* **1985**, *24*, 3067.

(3) Rawle, S. C.; Sewell, T. J.; Cooper, S. R. *Inorg. Chem.* **1987**, *26*, 3769.

(4) Bell, M. N.; Blake, A. J.; Gould, R. O.; Holder, A. J.; Hyde, T. I.; Lavery, A. J.; Reid, G.; Schröder, M. *J. Incl. Phenom.* **1987**, *5*, 169. Blake, A. J.; Gould, R. O.; Lavery, A. J.; Schroder, M. *Angew. Chem., Int. Ed. Engl.* **1986**, *25*, 274.

(5) Rawle, S. C.; Yagbasan, R.; Prout, K.; Cooper, S. R. *J. Am. Chem. Soc.* **1987**, *109*, 6181.

(6) Wieghardt, K.; Küppers, H. J.; Raabe, E.; Krüger, C. *Angew. Chem., Int. Ed. Engl.* **1986**, *25*, 1101.

(7) Blake, A. J.; Holder, A. J.; Hyde, T. I.; Roberts, Y. V.; Lavery, A. J.; Schröder, M. *J. Organomet. Chem.* **1987**, *323*, 261.

(8) Blower, P. J.; Clarkson, J. A.; Rawle, S. C.; Hartman, J. R.; Wolf, R. E., Jr.; Yagbasan, R.; Bott, S. G.; Cooper, S. R. *Inorg. Chem.* **1989**, *28*, 4040.

(9) Blake, A. J.; Gould, R. O.; Holder, A. J.; Hyde, T. I.; Lavery, A. J.; Odulate, M. O.; Schröder, M. *J. Chem. Soc., Chem. Commun.* **1987**, 118.

(10) Corfield, P. W. R.; Ceccarelli, C.; Glick, M. D.; Moy, I. W. Y.; Ochrymowycz, L. A.; Rorabacher, D. B. *J. Am. Chem. Soc.* **1985**, *107*, 2399.

(11) Rawle, S. C.; Cooper, S. R. *J. Chem. Soc., Chem. Commun.* **1987**, 308.

(12) Blake, A. J.; Gould, R. O.; Holder, A. J.; Hyde, T. I.; Schröder, M. *J. Chem. Soc., Dalton Trans.* **1988**, 1861.

(13) Blake, A. J.; Holder, A. J.; Hyde, T. I.; Schröder, M. *J. Chem. Soc., Chem. Commun.* **1989**, 1433.

(14) de Groot, B.; Loeb, S. H. *Inorg. Chem.* **1990**, *29*, 4084.

(15) Cooper, S. R. *Acc. Chem. Res.* **1989**, *21*, 141.

(16) Blake, A. J.; Holder, A. J.; Hyde, T. I.; Schröder, M. *J. Chem. Soc., Chem. Commun.* **1987**, 987.

(17) Grant, G. J.; Sanders, K. A.; Setzer, W. N.; VanDerveer, D. G. *Inorg. Chem.* **1991**, *30*, 4053. Sanders, K. A.; Grant, G. J.; Setzer, W. N. Re(III) and Pd(II) Complexes of Crown Thioethers. 201st National Meeting of the American Chemical Society, Atlanta, GA, 1991; Paper INOR 138.

0020-1669/92/1331-2663$03.00/0 © 1992 American Chemical Society